Journal of Applied Polymer Science

Isothermal Crystallization Kinetics and Mechanical Properties of Polycaprolactone Composites with Zinc Oxide, Oleic Acid, and Glycerol Monooleate

Burcu Alp,[1] Serap Cesur[2]
[1]Department of Chemical Engineering, Izmir Institute of Technology, Izmir, Turkey
[2]Department of Chemical Engineering, Ege University, Izmir, Turkey
Correspondence to: B. Alp (E-mail: burcualp@iyte.edu.tr)

ABSTRACT: The isothermal crystallization and mechanical behavior of polycaprolactone (PCL) with zinc oxide (ZnO) with oleic acid and glycerol monooleate (GMO) were studied. Theoretical melting points calculated by the Flory–Huggins and Thompson–Gibbs models were thoroughly compared with differential scanning calorimetry experimental observations. The isothermal crystallization kinetic parameters by Avrami analysis showed that crystallization was controlled by nucleation, crystal growth was spherical, and the nucleation type changed between thermal and athermal nucleation. X-ray diffraction showed that when the additives were used together both the crystal thickness and the degree of crystallinity increased. A multiple-response regression analysis was made with the ZnO, oleic acid, and GMO concentrations as variables and the crystallinity as output. Interaction parameters by the Pukanzky model were calculated from the tensile strength at the yield point and indicated that the addition of oleic acid or GMO improved the interface between the ZnO particles and PCL. © 2013 Wiley Periodicals, Inc. J. Appl. Polym. Sci. 130: 1259–1275, 2013

KEYWORDS: composites; crystallization; kinetics; mechanical properties

Received 3 August 2012; accepted 19 February 2013; published online 22 April 2013
DOI: 10.1002/app.39217

INTRODUCTION

Polycaprolactone (PCL) was one of the earliest polymers synthesized by the Carothers group in the early 1930s.[1] It is a biodegradable polyester with a high crystallinity and is produced from crude oil. Today, the importance of PCL has increased because it can be degraded by microorganisms. Attention was drawn to PCL because of its numerous advantages over other biopolymers in use at the time. These included its tailorable degradation kinetics and mechanical properties, ease of shaping and manufacturing that enable appropriate pore sizes conducive to tissue in-growth, controlled delivery of drugs contained within its matrix, and food packaging applications. Because PCL degrades at a slower rate than polyglycolide and poly(D,L-lactide) and its copolymers, it was originally used in drug-delivery devices that remained active for over 1 year and in slowly degrading suture materials. Furthermore, the fact that a number of drug-delivery devices fabricated with PCL already have U.S. Food and Drug Administration approval and CE-Mark registration gives these devices a faster avenue to the market.

Because of its low melting point and glass-transition temperature, PCL has a high crystallinity. Because of its potential applications, it can be mixed with other polymers, for example, polystyrene,[2] polyethylene,[3] polypropylene,[4] some inorganic additives such as forsterite,[5] nanohybrid–ZnAl-layered double hydroxide,[6] mixed-surface octyl/methoxyundecyl a–zirconium phosphonates,[7] iron phosphate,[8] isopropyl ortho titanate,[9] hydroxyapatite,[10] clay,[11–13] bamboo cellulose,[14] starch,[15,16] and functionalized single-walled carbon nanotubes.[17] For biodegradable polymeric composite applications, particles such as inorganic additives in PCL have been investigated extensively. There has been no study of the improvements in the crystallinity behavior of PCL with both organic and inorganic additives. Our aim, therefore, in this study was not only to control the crystallinity behavior of PCL with both inorganic additives such as zinc oxide (ZnO) and organic additives such as oleic acid and glycerol monooleate (GMO) but also to design composites with product properties for designed for certain application areas. ZnO particles are promising materials for future polymeric composites and blends used in food packaging, electrochemical biosensors, lasing luminescence, dental applications, medical uses, agricultural applications, drug release, and UV shielding materials; they also open new possible application fields with for polymers with improved thermal stability and mechanical properties.[18–22] Oleic acid[23] and GMO[24] offer better interfacial

properties to fluid–solid interfaces and the dispersion stability of inorganic particles in a polymer matrix.

EXPERIMENTAL

Materials

PCL (Aldrich; number-average molecular weight = 70,000–90,000) and dichloromethane (DCM; Merck) were used for the preparation of the polymeric films. ZnO (Merck), oleic acid (Riedel), and GMO (Kimsan A. Ş.) were used as additives to control the crystallization of PCL.

Preparation of the Composite Film

PCL (4.2 g) was dissolved in 70 cm^3 of DCM at room temperature, and the solution was mixed with a magnetic stirrer. Then, ZnO (0.1, 1, and 3 wt %) and oleic acid (1, 3, and 5 wt %) or GMO (1, 3, and 5 wt %) were added to the PCL solution and mixed for an additional 2 h. To obtain the composite film, 10 cm^3 of the mixture was poured into a Petri dish with a 10-cm diameter and then left for 12 h under a hood to evaporate the solvent from the film.

Analysis of the Structural Properties

The crystal structure of the composite films was identified by an X-ray diffractometer (Philips X'Pert-Pro) with Ni-filtered Cu Kα radiation (with a wavelength of 0.1546 nm) at a scanning rate of 6 min^{-1} with 2θ values ranging from 5 to 70° to determine the crystal structure of the samples. The degree of crystallinity of the composite films was calculated from the area of the crystal peak to the total area of the peak of the XRD pattern by the Gaussian function.

Measurement of the Crystallization Behavior by Differential Scanning Calorimetry (DSC)

The isothermal crystallization experiments were performed by DSC (TA Instruments Q10). For DSC analysis, samples (6 mg) were placed in a covered aluminum pan under a nitrogen atmosphere (40 cm^3/min) and heated at a rate of 10°C/min from room temperature to 100°C; they were then left for 10 min to delete the thermal memory. After that, they were rapidly cooled to 40°C with liquid nitrogen (at a cooling rate of 50°C/min) and then left for 30 min at that temperature to observe the isothermal crystallization. After the samples were cooled to 20°C at a 10°C/min cooling rate, they were heated again to 100°C at a 10°C/min heating rate.

Structure and Property Correlations

The evaluation of the results that depended on the ZnO, oleic acid, and GMO concentrations were performed with the Sigma Zone Doe Pro computer program. A multiple-response regression analysis was performed, and then the responses as functions of the additive concentration were examined by surface observation and the Pareto of regression coefficient. A regression analysis for experiments with coded variables with both linear and quadratic effects was done. In regression analysis, the p value represents the importance of the effect of the variable. If the p value is lower than 0.05, the effect of the variable is highly important. The F value represents the compatibility of the model with the experimental data. If the F value is equal to or greater than 6, the compatibility of the model is very good.[25] The regression equation is as follows:

$$Y = C_0 + C_1A + C_2B + C_3AB + C_4A^3 + C_5B^2 \quad (1)$$

where A represents the ZnO weight percentage and B represents either the oleic acid or GMO weight percentage. A regression analysis with Y as the degree of crystallinity and the Avrami exponent (n) was made in this study.

Analysis of the Mechanical Properties

The mechanical tensile tests were done according to ASTM D 882 with a strain rate of 500 mm/min with a tensile test analyzer (TA-XT Plus texture analyzer). Before the tests, the samples were kept at 23 ± 2°C and 50% relative humidity for 48 h.

RESULTS AND DISCUSSION

Hansen Solubility and Compatibility

The solubility parameters were examined to ensure the solubility of the polymer in the solvent casting solvent and the solubility of oleic acid and GMO in the polymer. The compatibility of the polymer and ZnO surfaces were checked with the solubility parameter criteria.

The solubility parameter concept has because been extended to various systems, including polar, polymer–solvent, and polymer–polymer systems. The solubility parameter model has been successful in describing the thermodynamic properties of solutions, especially when the component liquids are nonpolar or slightly polar.[26] The basis of these Hansen solubility parameters is that the total energy of vaporization of a liquid consists of several individual parts. These arise from the atomic dispersion forces, permanent dipole–permanent dipole forces (molecular), and hydrogen bonding (molecular and electron exchange). The total solubility parameters were estimated with eq. (2):

$$\delta = \sqrt{\delta_d^2 + \delta_p^2 + \delta_h^2} \quad (2)$$

where δ_d, δ_p, and δ_h are the dispersion, polar, and hydrogen-bonding partial solubility parameters, respectively. Also the partial solubility parameters of the polymer and pure organic compounds are estimated from the group contributions method. According to Stefanis and Panayiotou,[27] the equations for the estimation of the Hansen solubility parameters of oleic acid and GMO were done as follows:

$$\delta_d = \Sigma N_i C_i + 17.3231\ (\mathrm{MPa})^{1/2} \quad (3)$$

$$\delta_p = \Sigma N_i C_i + 7.3548\ (\mathrm{MPa})^{1/2} \quad (4)$$

$$\delta_h = \Sigma N_i C_i + 7.9793\ (\mathrm{MPa})^{1/2} \quad (5)$$

where C_i is the contribution of the group of type i that appears N_i times in the compound. The unit of the solubility parameters is $[\mathrm{MPa}]^{1/2}$ in the SI system of units.

The relative energy difference between the polymer and solvent is reflected by the RED number.[26] The RED number is defined the ratio of the solubility parameter distance (R_a) to the radius of the interaction sphere in Hansen space (R_o) for a selected polymer:

$$\text{RED} = \frac{R_a}{R_o} \tag{6}$$

The equation for the radius of the interaction sphere in Hansen space (R_o) for selected polymer's partial solubility parameter components is as follows:

$$R_o = 4\delta_d^2 + \delta_p^2 + \delta_h^2 \tag{7}$$

The equation for R_a between two materials on the basis of their respective partial solubility parameter components is as follows:

$$R_a^2 = 4(\delta_{d2} - \delta_{d1})^2 + (\delta_{p2} - \delta_{p1})^2 + (\delta_{h2} - \delta_{h1})^2 \tag{8}$$

It is obvious that the solubility, or high affinity, requires that R_a be less than R_o. If the RED number is equal to zero, it means that R_a is equal to zero and there are no energy differences between the polymer and solvent; if it is smaller than 1, there is a high affinity; and if it is equal to or greater than 1, there is a lower affinity.

The calculated solubility parameters are given in Table I; the distance between PCL and the selected solvent, organic and inorganic additives, R_a, and RED numbers (the R_o value of PCL was calculated to be 36.27) are given in Table II. The calculated interaction spheres for PCL, DCM, ZnO, oleic acid, and GMO are shown in Figure 1(a,b). According to the results obtained, PCL is soluble in DCM, oleic acid, and glycerol monooleate and compatible with ZnO because all of the RED number values were smaller than 1.[26]

Effect of Additives on the Crystal Structure

With the Debye–Scherrer equation [eq. (9)], the crystal thickness from the X-ray analysis of the PCL composite films was calculated:[28]

$$t = \frac{\kappa\lambda}{B\cos\theta_B} \tag{9}$$

where κ is a dimensionless constant that may range from 0.89 to 1.39, depending on the specific geometry of the scattering objects. For a perfect two-dimensional lattice, where every point on the lattice emits a spherical wave, numerical calculations yield a lower bound of 0.89 for κ. A cubic three-dimensional crystal is best described by $\kappa = 0.94$, whereas analytical calculations for a perfectly spherical object yield $\kappa = 1.33$. κ was taken as 0.9 in this study. B is a measure of the peak width, the full width at half-maximum at 2θ.

Table I. Calculated Hansen Solubility Parameters $(\text{MPa})^{1/2}$

Substance	δ_d	δ_p	δ_h	δ_T
PCL	17.30	9.30	7.00	20.82
DCM	18.20	6.30	6.10	20.20
Oleic acid	18.90	2.90	5.20	19.86
Glycerol monooleate	16.10	7.50	15.90	23.80
ZnO	16.90	7.80	10.60	21.40

Table II. Calculated Solubility Parameter Distance between PCL and Selected Solvents, Organic and Inorganic Additives, R_a, and RED Number

Substance	R_a	RED number
PCL–DCM	3.66	0.10
PCL–oleic acid	7.44	0.20
PCL–glycerol monooleate	9.33	0.25
PCL–ZnO	3.91	0.10

The R_o value of PCL was calculated as 36.27.

From the X-ray diffraction pattern, the calculation for *d*-spacing (also called *interplanar spacing* or *lattice plane spacing*), d_{hkl}, is simple in the case of crystals with orthogonal axes. The unit cell of PCL was found by Bittiger and Marchessault[29] to be orthorhombic with dimensions of $a = 7.496 \pm 0.002$, $b = 4.974 \pm 0.001$, and $c = 17.297 \pm 0.023$ Å. For the orthorhombic unit cell, d_{hkl} was calculated with eq. (10).[30] In the calculation of the *d*-spacing of the (111) planes of the PCL films, the h, k, and l values were taken as 1:

$$d_{hkl} = \frac{1}{\sqrt{\left(\frac{h}{a}\right)^2 + \left(\frac{k}{b}\right)^2 + \left(\frac{l}{c}\right)^2}} \tag{10}$$

The compositions and codes of the 28 prepared composite films are given in Table III, where the letter *Z* indicates ZnO, *O* indicates oleic acid, *G* indicates GMO, and the number indicates the weight percentage of additives in the composites. The maximum peaks were observed near 2θ values of 21.8 and 24.08, as shown in Figure 2(a–d) and were due to the presence of PCL crystals in the samples. The crystal thicknesses, calculated at a maximum peak of 2θ, are given in Table II. It was observed from Figure 3(a,b) that when additives were used alone, both the crystal thickness and the degree of crystallinity decreased at low concentrations and increased at high concentrations. However, when the additives were used together, both the crystal thickness and degree of crystallinity increased except with the addition of 3 wt % oleic acid. Because ZnO acted as nucleating agent, oleic acid and GMO acted as plasticizers. A similar observation was made when clay was used.[31–33]

The measured unit cell parameters determined by eq. (9) were quite consistent with the orthorhombic unit cell of PCL determined from the X-ray data; the peak observed at a 2θ value of 21.803 was the (111) lattice plane, and the peak observed at a 2θ value of 24.08 was the (100) lattice plane.

Effect of the Additives on the Melting Behavior

The crystallization rate is a function of the crystallization temperature, glass-transition temperature, and melting temperature (T_m). Between the glass transition temperature and T_m, the crystallization rate has a maximum value.[34] T_m is effected by the presence of solvents (i.e., oleic acid and glycerol monooleate) and the size of the crystals. Thus, it was necessary to check the predicted and experimental T_m's.

Applied Polymer SCIENCE

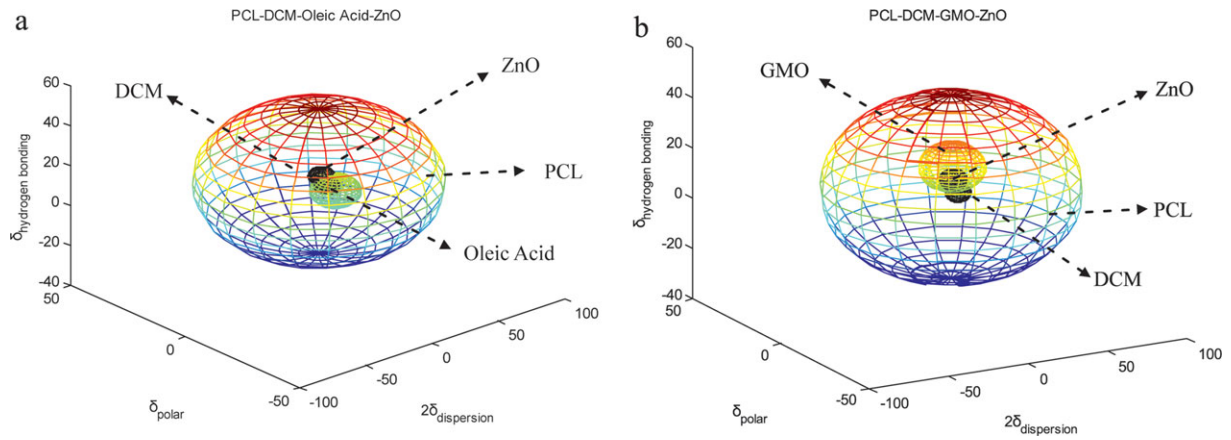

Figure 1. Calculated interaction spheres of (a) PCL, DCM, oleic acid, and ZnO and (b) PCL, DCM, GMO, and ZnO. [Color figure can be viewed in the online issue, which is available at wileyonlinelibrary.com.]

Table III. Sample Compositions, Degrees of Crystallinity of the Composite Films by XRD Patterns, and Calculated Crystal Thicknesses Observed at 2θ

Sample	wt %			Degree of crystallinity by XRD (%)	2θ (°)	Crystal thickness (nm)
	ZnO	Oleic acid	GMO			
Neat PCL	0	0	0	58.82	21.61	27.02
PCL-O1	0	1	0	57.14	21.38	12.33
PCL-O3	0	3	0	53.31	21.53	20.54
PCL-O5	0	5	0	47.99	21.55	42.32
PCL-G1	0	0	1	53.00	21.23	35.10
PCL-G3	0	0	3	53.00	21.18	30.48
PCL-G5	0	0	5	51.00	21.64	35.13
PCL-Z0.1	0.1	0	0	45.81	21.24	19.26
PCL-Z0.1-O1	0.1	1	0	44.86	21.35	27.00
PCL-Z0.1-O3	0.1	3	0	48.16	21.32	27.00
PCL-Z0.1-O5	0.1	5	0	42.66	21.49	27.01
PCL-Z0.1-G1	0.1	0	1	50.70	21.58	20.23
PCL-Z0.1-G3	0.1	0	3	55.00	21.54	35.11
PCL-Z0.1-G5	0.1	0	5	53.00	21.38	30.50
PCL-Z1	1	0	0	54.21	21.63	30.99
PCL-Z1-O1	1	1	0	62.22	21.49	42.32
PCL-Z1-O3	1	3	0	55.37	21.95	24.67
PCL-Z1-O5	1	5	0	53.72	21.64	27.39
PCL-Z1-G1	1	0	1	53.00	21.48	30.49
PCL-Z1-G3	1	0	3	49.00	21.03	22.04
PCL-Z1-G5	1	0	5	47.00	21.55	35.12
PCL-Z3	3	0	0	50.18	21.35	14.08
PCL-Z3-O1	3	1	0	48.39	21.21	30.48
PCL-Z3-O3	3	3	0	45.41	21.20	20.22
PCL-Z3-O5	3	5	0	47.24	21.27	51.54
PCL-Z3-G1	3	0	1	53.00	21.46	30.50
PCL-Z3-G3	3	0	3	51.00	20.95	30.47
PCL-Z3-G5	3	0	5	50.00	21.27	51.54

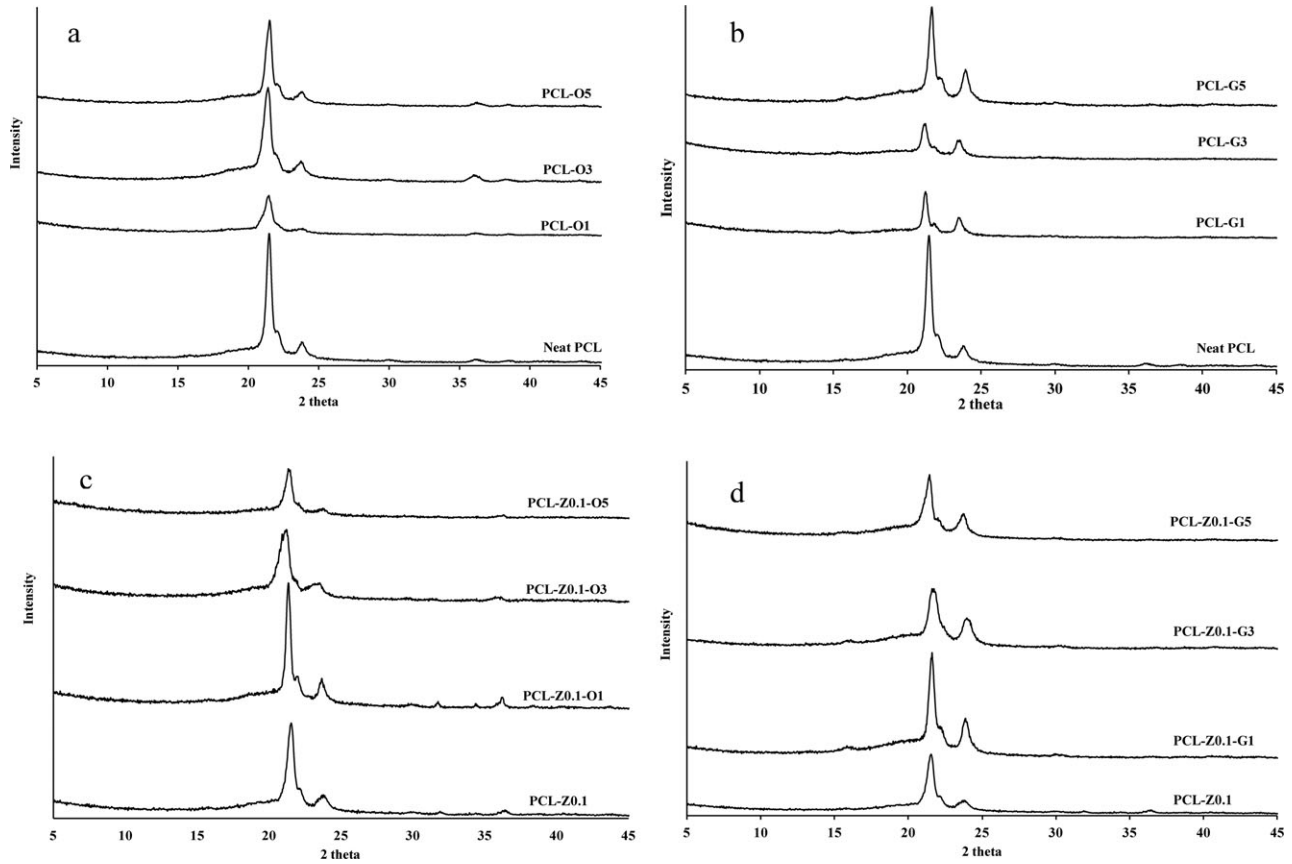

Figure 2. XRD patterns for the effects of the additives on the crystal structure of the composite films: (a) oleic acid effect, (b) GMO effect, (c) ZnO–oleic acid effects, and (d) ZnO–GMO effects.

The isothermal DSC heating and cooling profile for the PCL-Z0.1-G3 sample is shown in Figure 4. The degree of crystallinity (X_c) of the samples from DSC melting peaks were determined as follows:

$$X_c(\%) = \frac{\Delta H_m}{w\Delta H_f^0} \times 100 \tag{11}$$

where ΔH_m is the melting enthalpy of the samples (J/g) and ΔH_f^0 is the heat of the fusion of PCL at 100% crystallinity (139.5 J/g),[35] and w is the weight fraction of PCL in the composite film.

Polymer crystals are lamella-shaped, and their twofold surfaces greatly dominate the total surface energy term. The Thompson–Gibbs equation predicts a linear relationship between T_m and the reciprocal of crystal thickness:[34]

$$T_m = T_m^0\left(1 - \frac{2\sigma}{L_c\rho_c\Delta H_f^0}\right) \tag{12}$$

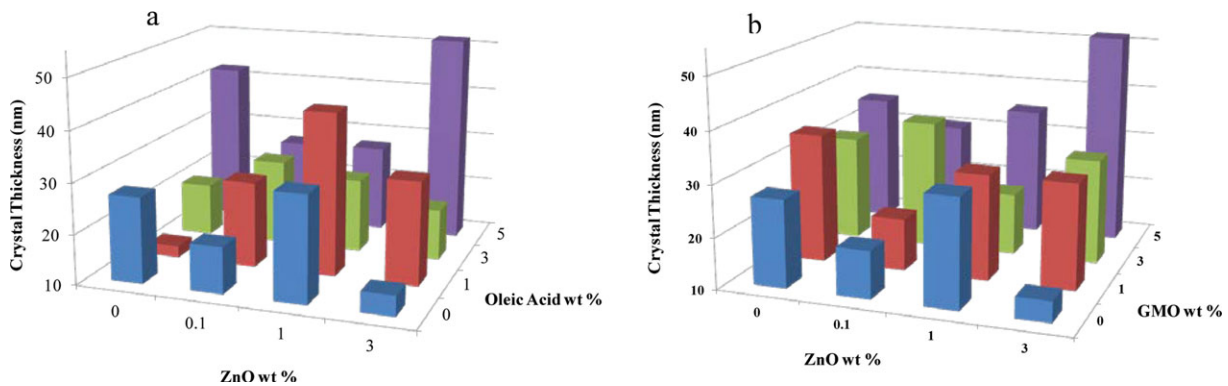

Figure 3. Effect of the additive concentration on the crystal thickness of the composite films: (a) ZnO–oleic acid and (b) ZnO–GMO. [Color figure can be viewed in the online issue, which is available at wileyonlinelibrary.com.]

Applied Polymer SCIENCE

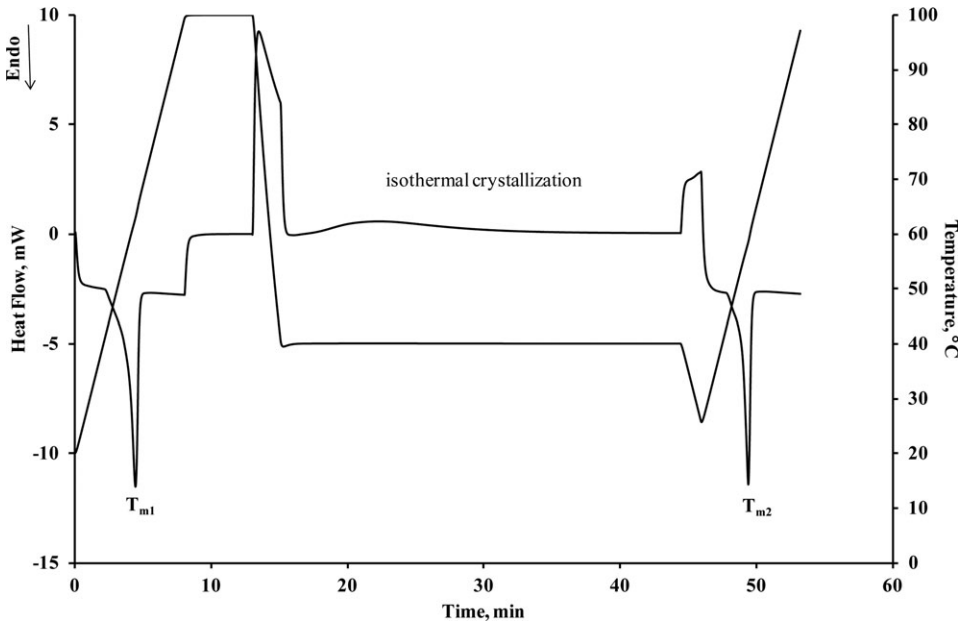

Figure 4. Isothermal DSC heating and cooling profiles of the PCL–Z0.1–G3 sample.

where σ is the fold surface free energy, T_m^0 is the equilibrium melting temperature, ρ_c is the number of segments per volume in the crystalline state, and L_c is the thickness of the lamellar crystals. The L_c values calculated from the XRD pattern were used. In addition, the following values from the literature for the parameters of PCL were used:[36] $\sigma = 8.23 \times 10^{-3}$ J/m, T_m^0

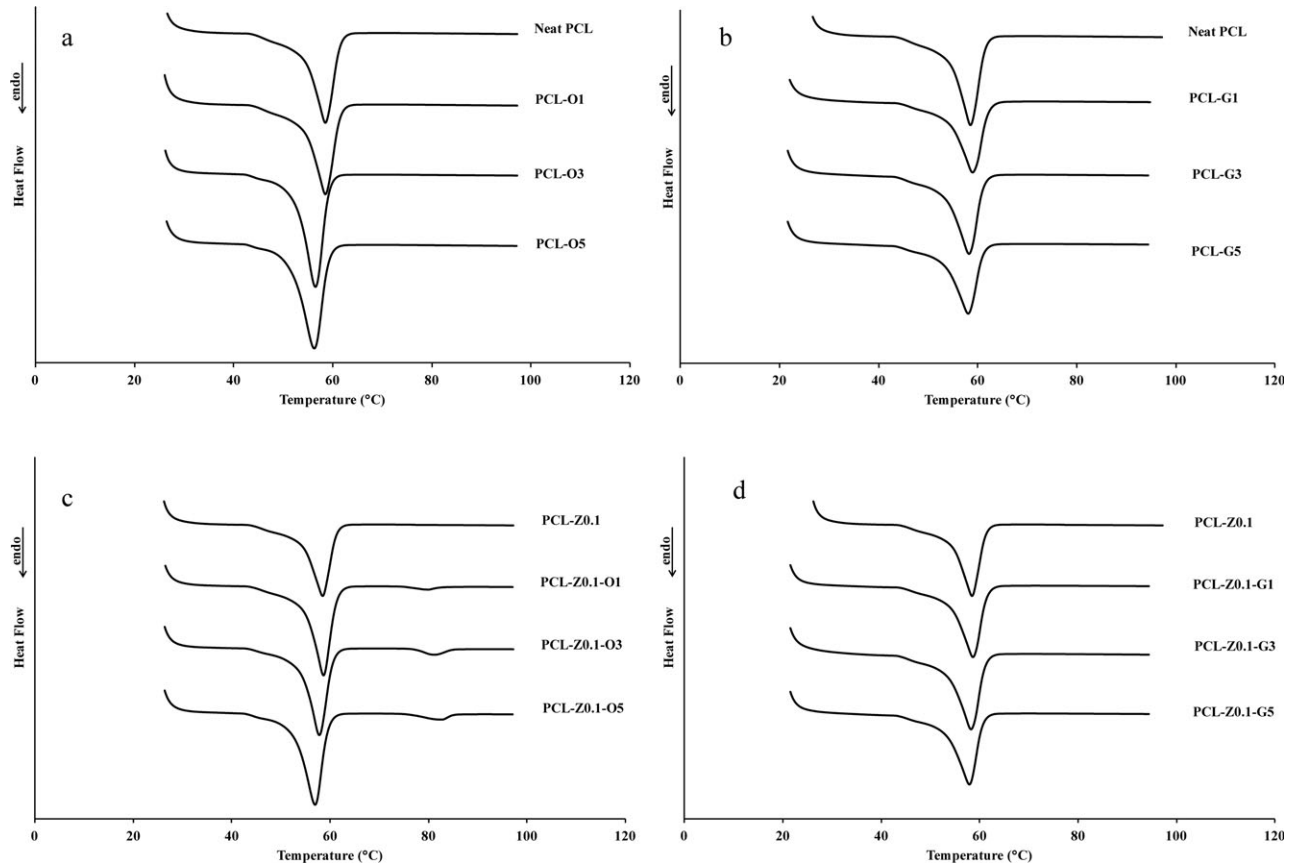

Figure 5. Effect of the additives on the melting behavior of the composite films during the second heating: (a) oleic acid effect, (b) GMO effect, (c) ZnO–oleic acid effect, and (d) both ZnO–GMO effect.

Table IV. Observed and Calculated T_m's, Standard Deviation, Melting Enthalpy, and Degree of Crystallinity of the Samples for First Melting by DSC Analysis

	First T_m (°C)						
		Calculated					
				Standard deviation (%)			
Sample	Observed	Flory Huggins equation	Thompson Gibbs equation	Flory–Huggins equation	Thompson–Gibbs equation	ΔH_1 (J/g)	X_{c1} (%)
Neat PCL	62.89	–	64.90	–	3.10	80.65	57.81
PCL-O1	61.83	65.78	63.60	6.00	2.78	88.94	63.12
PCL-O3	61.07	65.34	64.56	6.54	5.40	92.75	64.49
PCL-O5	60.75	64.92	65.30	6.43	6.97	92.24	62.82
PCL-G1	61.00	65.81	65.16	7.31	6.38	64.32	45.65
PCL-G3	60.18	65.46	65.03	8.07	7.45	66.15	46.00
PCL-G5	59.88	65.14	65.16	8.08	8.10	63.69	43.37
PCL-Z0.1	61.53	—	64.46	—	4.55	77.12	55.23
PCL-Z0.1-O1	63.09	65.78	64.90	4.09	2.79	83.43	59.15
PCL-Z0.1-O3	62.09	65.34	64.90	4.98	4.33	83.75	58.17
PCL-Z0.1-O5	61.13	64.92	64.90	5.84	5.81	83.92	57.09
PCL-Z0.1-G1	61.38	65.81	64.54	6.73	4.89	75.08	53.23
PCL-Z0.1-G3	60.42	65.46	65.16	7.70	7.27	78.17	54.30
PCL-Z0.1-G5	59.22	65.14	65.03	9.09	8.93	65.71	44.70
PCL-Z1	64.24	—	65.04	—	1.24	83.06	58.95
PCL-Z1-O1	63.42	65.78	65.30	3.58	2.88	77.39	54.37
PCL-Z1-O3	62.69	65.34	64.80	4.05	3.25	82.85	57.02
PCL-Z1-O5	60.80	64.91	64.92	6.34	6.34	90.52	61.00
PCL-Z1-G1	60.63	65.81	65.03	7.87	6.76	67.35	47.75
PCL-Z1-G3	59.39	65.46	64.66	9.27	8.14	65.35	45.39
PCL-Z1-G5	60.23	65.14	65.16	7.53	7.56	67.72	46.07
PCL-Z3	63.25	—	63.90	—	1.01	74.67	51.92
PCL-Z3-O1	63.44	65.77	65.03	3.54	2.44	80.86	55.65
PCL-Z3-O3	64.83	65.32	64.53	0.76	-0.46	67.64	45.58
PCL-Z3-O5	63.85	64.89	65.43	1.61	2.41	64.05	42.24
PCL-Z3-G1	60.78	65.81	65.03	7.64	6.53	70.52	48.53
PCL-Z3-G3	59.35	65.45	65.03	9.31	8.73	71.36	48.08
PCL-Z3-G5	60.08	65.12	65.43	7.74	8.17	63.00	41.55

= 66°C, $\Delta H = 2.97 \times 10^{-20}$ J, and $\rho_c = 6.34 \times 10^{27}$ m^{-3}. In addition, the addition of a solvent to the polymer decreased T_m in a manner that was predictable by the Flory–Huggins equation:

$$\frac{1}{T_m} - \frac{1}{T_m^0} = \frac{R}{\Delta H_u}\frac{V_u}{V_i}(\upsilon_1 - \chi\upsilon_1^2) \quad (13)$$

where V_u is the molar volume of the polymer repeat unit, ΔH_u is the heat of fusion per polymer repeat unit, V_1 is the molar volume of the solvent, υ_1 is the volume fraction of the solvent, R is the gas constant, T_m^0 is the melting temperature of the pure polymer, and χ is the polymer–solvent interaction parameter and is calculated with eq. (14):

$$\chi = \beta_1 + \frac{v_1}{RT}(\delta_1 - \delta_2)^2 \quad (14)$$

where δ_1 and δ_2 are the solubility parameters of the solvent and the polymer, respectively, and β_1 is the lattice constant, usually 0.35 ± 0.1.

The T_m and degree of crystallinity values of the samples were calculated from melting endotherms obtained by the first and the second heating runs of the samples. The melting endotherms of some of the PCL films during the second heating are given in Figure 5(a–d). In some of the PCL films that were prepared for ZnO and oleic acid, after the first and second melting peaks, another small melting peak was observed. These small

Table V. Observed and Calculated T_m, Standard Deviation, ΔH, and Degree of Crystallinity Values of the Samples for the Second Melting by DSC Experiments

	T_m (°C)						
		Calculated					
				Standard deviation (%)			
Sample	Observed	Flory–Huggins equation	Thompson–Gibbs equation	Flory–Huggins equation	Thompson–Gibbs equation	ΔH_2 (J/g)	X_{c2} (%)
Neat PCL	58.48	—	64.90	—	9.90	59.77	42.85
PCL-O1	57.88	65.78	63.60	12.01	8.99	65.75	46.66
PCL-O3	56.43	65.34	64.56	13.64	12.59	68.04	47.31
PCL-O5	56.34	64.92	65.30	13.22	13.72	66.14	45.04
PCL-G1	58.97	65.81	65.16	10.40	9.49	54.15	38.43
PCL-G3	58.25	65.46	65.03	11.02	10.42	52.64	36.60
PCL-G5	58.09	65.14	65.16	10.83	10.85	50.41	34.33
PCL-Z0.1	58.42	—	64.46	—	9.37	52.39	37.52
PCL-Z0.1-O1	58.69	65.78	64.90	10.78	9.57	60.04	42.57
PCL-Z0.1-O3	57.81	65.34	64.90	11.53	10.93	61.44	42.68
PCL-Z0.1-O5	57.02	64.92	64.90	12.17	12.15	60.62	41.24
PCL-Z0.1-G1	58.59	65.81	64.54	10.97	9.21	58.05	41.16
PCL-Z0.1-G3	58.30	65.46	65.16	10.94	10.52	53.09	36.88
PCL-Z0.1-G5	57.84	65.14	65.03	11.21	11.05	53.21	36.20
PCL-Z1	58.91	—	65.04	—	9.43	58.43	41.47
PCL-Z1-O1	58.53	65.78	65.30	11.02	10.37	55.86	39.24
PCL-Z1-O3	57.56	65.34	64.80	11.90	11.17	61.46	42.30
PCL-Z1-O5	56.25	64.91	64.92	13.35	13.35	66.00	44.47
PCL-Z1-G1	58.14	65.81	65.03	11.66	10.59	54.40	38.57
PCL-Z1-G3	58.18	65.46	64.66	11.12	10.02	53.73	37.32
PCL-Z1-G5	58.00	65.14	65.16	10.96	10.98	52.21	35.52
PCL-Z3	58.74	—	63.90	—	8.07	53.38	37.12
PCL-Z3-O1	58.63	65.77	65.03	10.86	9.84	56.32	38.76
PCL-Z3-O3	58.21	65.32	64.53	10.89	9.80	50.31	33.90
PCL-Z3-O5	58.44	64.89	65.43	9.94	10.68	46.91	30.94
PCL-Z3-G1	58.25	65.81	65.03	11.48	10.42	53.90	37.09
PCL-Z3-G3	57.98	65.45	65.03	11.41	10.84	50.09	33.75
PCL-Z3-G5	58.11	65.12	65.43	10.76	11.18	57.21	37.73

melting peaks were thought to belong to zinc oleate covering the ZnO particles.[37] Zinc oleate is expected to form at the surface of the ZnO particles as a thin layer. When ZnO particles were coated with zinc oleate, their dispersion in the PCL matrix was better.[38]

The enthalpy, degree of crystallinity, and T_m's observed and calculated with both the Thompson–Gibbs model [eq. (12)] and Flory–Huggins model [eq. (13)] are given in Tables IV and V for the first and second melting endotherms, respectively. The calculated T_m's from the two different models were close to each other. The first T_m values of the composite films were higher than the second melting values because of the effect of the solvent that might have remained in the film, and because of the different crystallization mechanisms, the melting of crystals formed from the solution, and the melting of crystals formed from the bulk of the composite films. However, the T_m's calculated from the two different models were closer to the first T_m than to the second T_m. The addition of a solvent to a polymer decreases its T_m.[39] This situation was observed in the second melting process, which was the melting of the polymer crystallized from the polymer melt. Both oleic acid and GMO decreased the first and second T_m values, whereas ZnO slightly increased it.

The degree of crystallinity values of the composite films that were calculated from the first melting peak were higher than the values calculated from the second melting peak. This was because of the different crystallization mechanisms due to the melting from a solution and the melting from the bulk of composite films. We observed that the degree of crystallinity percentage of composite films increased with the addition of oleic acid and decreased with the addition of GMO and ZnO.

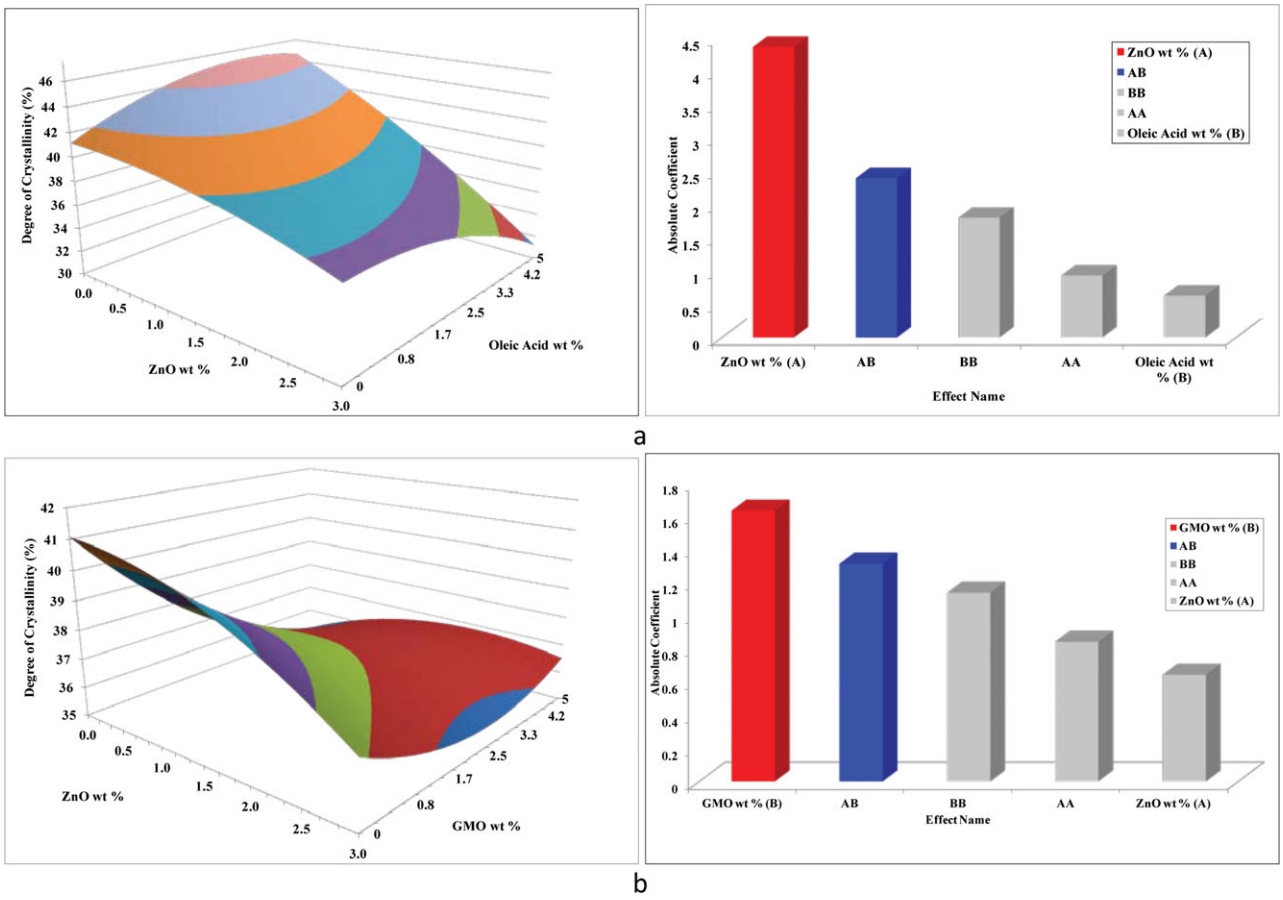

Figure 6. Regression analysis of the degree of crystallinity (%) of the composite films from the second melting depending on the additive concentration: (a) ZnO–oleic acid and (b) ZnO–GMO. [Color figure can be viewed in the online issue, which is available at wileyonlinelibrary.com.]

The regression analysis of the degree of crystallinity percentage from the second melting of the PCL composite films is shown in Figure 6. The degree of crystallinity percentage decreased with GMO and ZnO and increased with oleic acid. For the ZnO–oleic acid-doped composite films, ZnO was the dominant affecting parameter, but GMO was the more dominant affecting parameter for the ZnO–GMO-doped composite films from the Pareto plot. The regression equation constants are given in Table VI with the p value, which is the measure of the significance of an effect. A p value of less than 0.05 is considered highly significant, and the F value, if greater than 6, indicates a significant model for prediction.

Effect of the Additives on the Crystallization Behavior

Avrami Analysis. The crystallization kinetic parameters were obtained from the isothermal crystallization peak area at 40°C with the Avrami model. The Avrami model[40] was used to analyze the crystallization rates of the samples and is given in eq. (15):

$$X_t = 1 - \exp(-kt^n) \tag{15}$$

where X_t is the relative crystallinity; n is the Avrami constant, which depends on the mechanism of nucleation and the crystal growth; t is the real time of crystallization; and k is the crystallization rate constant and involves both nucleation and growth rate parameters.

X_t can be defined as a function of time in the following form:

$$X_t = \frac{\int_0^t \left(\frac{dH}{dt}\right) dt}{\int_0^\infty \left(\frac{dH}{dt}\right) dt} \tag{16}$$

Table VI. Values Regression Equation Constants for the Degree of Crystallinity

	X_{c2} (%)			
Constant	Oleic acid	p	GMO	p
C_0	42.99	7.47×10^{-10}	37.2	2.29×10^{-11}
C_1	−3.95	4.5×10^{-4}	−0.64	0.26
C_2	0.38	0.52	−1.63	0.02
C_3	1.07	0.05	−0.84	0.08
C_4	−2.59	0.62	1.31	0.48
C_5	−1.81	0.29	1.14	0.29
R^2	0.73		0.67	
Standard error	2.79		1.72	
F	6.10	4.15		

If the p value is lower than 0.05, the effect of the variable is highly important. The F value represents the compatibility of the model with the experimental data. If the F value is equal to or greater than 6, the compatibility of the model is very good.

Applied Polymer SCIENCE

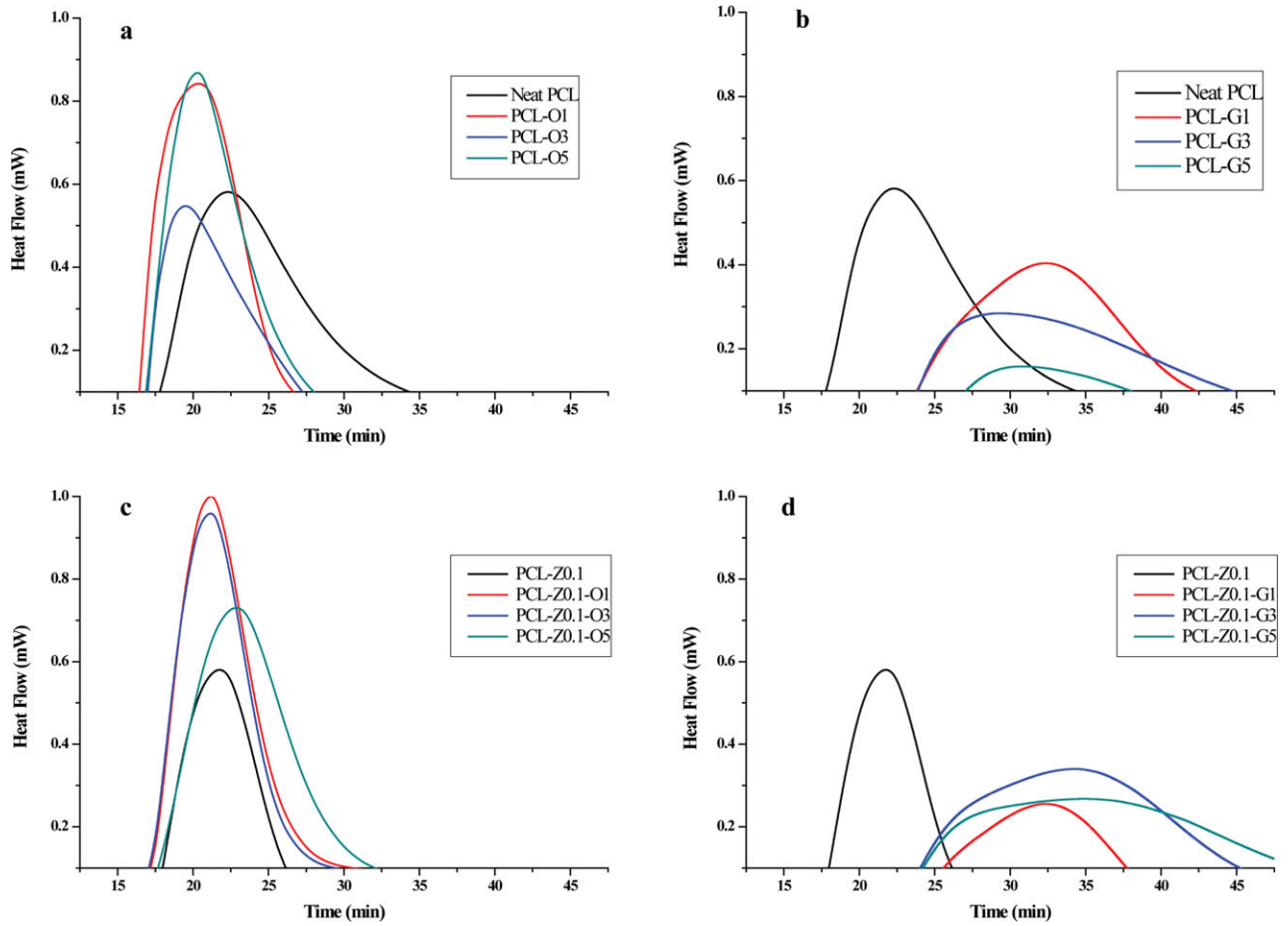

Figure 7. Effect of additives on the isothermal crystallization of the composite films at 40°C: (a) oleic acid effect, (b) GMO effect, (c) ZnO–oleic acid effect, and (d) ZnO–GMO effect. [Color figure can be viewed in the online issue, which is available at wileyonlinelibrary.com.]

where H is the crystallization enthalpy during the infinitesimal time interval dt and ∞ is the time at the end of crystallization.

Equation (14) can be linearized as follows:

$$\mathrm{In}[-\mathrm{In}(1 - X_t) = \mathrm{In}\ k + n\ \mathrm{In}\ t] \tag{17}$$

When $\ln[-\ln(1 - X_t)]$ versus $\ln t$ is plotted at a given crystallization temperature, a straight line should be obtained to determine the kinetic n values. The slope of the line is equal to n, and the intercept is $\ln k$. Also, k can be determined from the crystallization halftime, which is defined as the time taken for the crystallinity of the sample to reach a value of 50% of X_t:

$$k = \frac{(\mathrm{In2})}{t_{1/2}^{n}} \tag{18}$$

The isothermal crystallization exotherms for some PCL films are shown in Figure 7(a–d). The kinetics parameters were obtained from these isothermal exotherms with the Avrami model and are summarized in Table VII. The X_t–time (t) plots of the samples are shown in Figure 8(a–d). All of the X_t curves had the same characteristic sigmoidal shape with time at the isothermal crystallization temperature (40°C). Each curve showed a linear part considered to be the primary crystallization; later, a second nonlinear part deviated off slightly and was considered to be due to secondary crystallization, which was caused by spherulite growth. As a matter of fact, the Avrami model was valid for the linear part of these curves. Di Maio et al.[41] reported that the isothermal crystallization of PCL/clay nanocomposites at different clay concentrations and showed that the well-dispersed organoclay platelets acted as nucleating agents in the PCL matrix, remarkably reducing the crystallization half-time ($t_{1/2}$). This effect was the maximum for the nanocomposite with 0.4 wt % clay, which showed the highest crystallization rate. In this study, ZnO addition also decreased $t_{1/2}$ and, therefore, the whole crystallization time.

The effect of additives on the Avrami plots of $\ln[-\ln(1 - X_t)]$ versus $\ln t$ of the PCL composite films are shown in Figure 9(a–d). The values of n and k obtained with eq. (18) from the slope and intercept of the best fitting line, along with $R^2 = 0.99$, are reported in Table VIII. For isothermal crystallization, only two cases are of importance, namely, the case where the nuclei are there from the beginning and the case where the nucleation rate is constant and finite. In the first case, one has a fixed number density of athermal nuclei or of heterogeneous nuclei, the latter being introduced by nucleation agents or impurities. In the second case, the melt is clean, and sporadic nucleation of thermal nuclei occurs. The critical point in both cases is the choice of

Table VII. Heat of Crystallization and Crystallization Kinetic Parameters Based on the Avrami Analysis with $R^2 = 0.99$

				k (min^{-1})	
Sample	ΔH_c (J/g)	$t_{1/2}$ (min)	n	ln $2/t_{1/2}^n$	Intercept from the Avrami plot
Neat PCL	52.19	7.13	2.05	0.0124	0.0108
PCL-O1	63.21	4.68	1.86	0.0393	0.0382
PCL-O3	62.58	6.83	1.86	0.0194	0.0175
PCL-O5	61.57	5.25	2.01	0.0247	0.0214
PCL-G1	42.33	10.27	2.37	0.0028	0.0028
PCL-G3	48.56	10.63	2.05	0.0055	0.0053
PCL-G5	49.94	10.93	2.05	0.0051	0.0051
PCL-Z0.1	53.73	6.41	2.32	0.0093	0.0082
PCL-Z0.1-O1	56.63	5.08	2.42	0.0136	0.0119
PCL-Z0.1-O3	56.58	5.00	2.27	0.018	0.0157
PCL-Z0.1-O5	58.89	7.23	2.53	0.0046	0.0043
PCL-Z0.1-G1	69.97	10.47	2.02	0.006	0.0063
PCL-Z0.1-G3	30.47	11.50	2.17	0.0035	0.0033
PCL-Z0.1-G5	42.09	12.04	2.10	0.0037	0.0038
PCL-Z1	58.27	4.01	2.73	0.0156	0.0137
PCL-Z1-O1	54.17	4.96	2.36	0.0158	0.0129
PCL-Z1-O3	55.97	3.68	2.52	0.026	0.0237
PCL-Z1-O5	66.71	9.33	2.16	0.0056	0.0053
PCL-Z1-G1	47.30	7.46	2.70	0.0031	0.0028
PCL-Z1-G3	58.95	9.64	2.33	0.0035	0.0036
PCL-Z1-G5	43.47	11.61	2.16	0.0035	0.0037
PCL-Z3	52.05	3.95	2.50	0.0223	0.0182
PCL-Z3-O1	57.50	7.71	2.56	0.0037	0.0033
PCL-Z3-O3	48.46	10.08	2.77	0.0012	0.0011
PCL-Z3-O5	45.52	4.81	2.67	0.0104	0.0096
PCL-Z3-G1	43.34	8.45	2.06	0.0085	0.0085
PCL-Z3-G3	56.70	9.37	2.35	0.0036	0.0036
PCL-Z3-G5	52.71	8.31	2.57	0.003	0.0027

time zero. The time interval needed for quenching must be very short compared with the time required for the crystallization process proper. The various n values are associated with different nucleation types and crystal geometries.[42,43] The n values change between 1.86 and 2.77. These show that the crystallization is controlled by nucleation, and the crystals have a spherical structure. The nucleation type changes between the thermal and athermal nucleation processes, and these are followed by three-dimensional spherulite growth.[41,42]

The n values of the composite films, expressed by surface characteristics and Pareto plots are shown in Figure 10(a,b). The surface graphs have saddle shapes. It is shown that the ZnO particles acted as a nucleation agent and, therefore, led to a defective crystal structure in the PCL matrix. n increased with ZnO to a maximum point and then decreased; however, it only slightly decreased with oleic acid and GMO. According to the Pareto analysis, the affecting parameter was ZnO for all of the composite films.

The growth rate k decreased with ZnO and slightly increased with the oleic acid concentration for the ZnO–oleic acid-doped composite films, whereas it increased with ZnO for the ZnO–GMO-doped composite films. The addition of a small amount of ZnO has an increasing effect on n, but when the amount of ZnO increases, the behavior became opposite. Researchers have remarked strongly that at very low levels of inorganic additives, such as clay, hydroxyapatite, and starch, the crystallization kinetics of the nanocomposites were dramatically increased with respect to extruded pure material.[11,14,41,44–46] This behavior is commonly observed in particulate-filled polymers. At low filler concentrations, the filler polymer interfaces act as a heterogeneous nucleating agent. In the crystallization kinetics at higher filler contents, the diffusion of polymer chains to the growing crystallites is blocked, and the overall crystallization rate is reduced with increasing nucleation rate.

Effect of the Additives on the Mechanical Behavior

Interfacial interaction between the fillers and matrix is an important factor affecting the mechanical properties of composites.[47] Thus, the theoretical tensile yield strength and ultimate tensile strength of the composites were modeled for the cases of

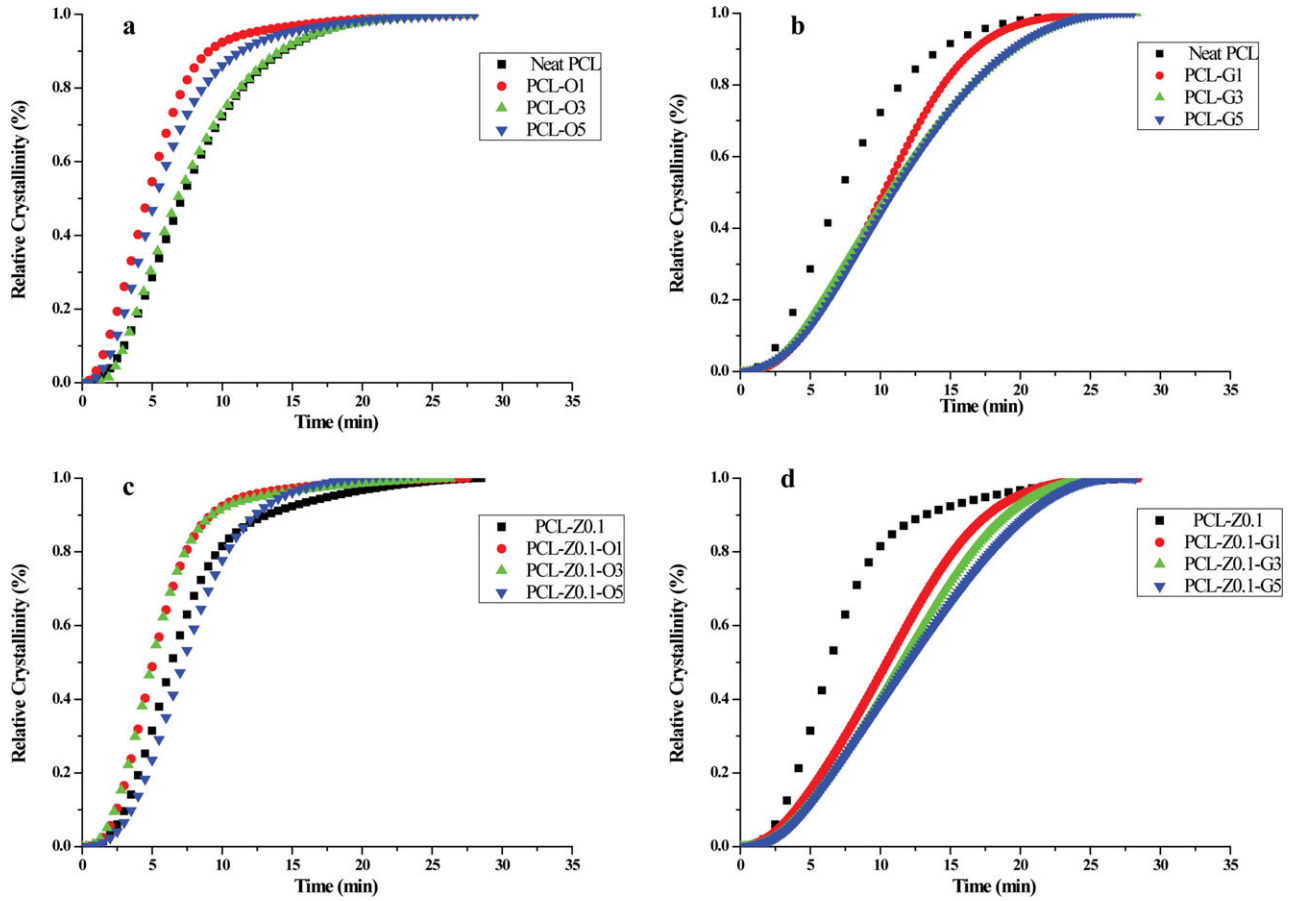

Figure 8. Effect of the additives on the X_t variation of the composite films: (a) oleic acid effect, (b) GMO effect, (c) ZnO–oleic acid effect, and (d) ZnO–GMO effect of exotherms of the composite films. [Color figure can be viewed in the online issue, which is available at wileyonlinelibrary.com.]

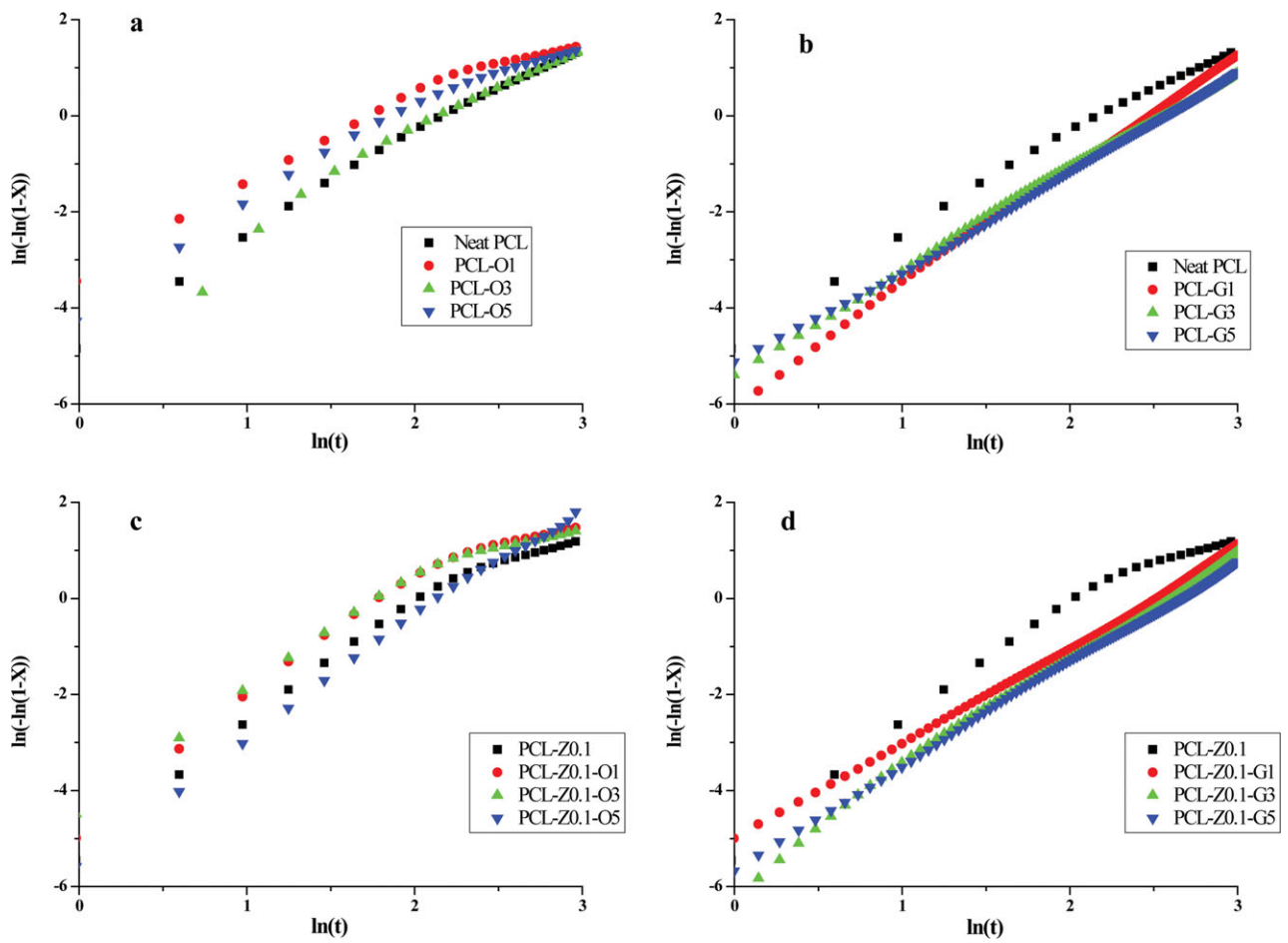

Figure 9. Effect of the additives on the Avrami plots of $\ln[-\ln(1 - X_t)]$ versus $\ln t$ of the composite films: (a) oleic acid effect, (b) GMO effect, (c) ZnO–oleic acid effect, and (d) ZnO–GMO effect. [Color figure can be viewed in the online issue, which is available at wileyonlinelibrary.com.]

Table VIII. Values of the Regression Equation Constants for n

	n			
Constant	Oleic acid	p	GMO	p
C_0	2.5546	2.87×10^{-8}	2.5007	4.36×10^{-9}
C_1	0.2496	0.08	0.1350	0.05
C_2	−0.0002	0.99	−0.0554	0.43
C_3	−0.2018	0.75	−0.3105	0.29
C_4	0.0367	0.25	0.0883	0.04
C_5	0.0385	0.79	0.0805	0.51
R^2	0.5366		0.5514	
Standard error error	0.2440		0.1966	
F	2.31			2.45

If the p value is lower than 0.05, the effect of the variable is highly important. The F value represents the compatibility of the model with the experimental data. If the F value is equal to or greater than 6, the compatibility of the model is very good.

adhesion and no adhesion between the filler particles and the matrix. The Pukanzky model describes the effects of composition and the interfacial interaction on the tensile yield stress of particulate-filled polymers. The parameter B is an interaction parameter that is related to the macroscopic characteristics of the filler–matrix interface and the interphase:

$$\sigma_{yc}/\sigma_{ym} = \frac{1-\phi_f}{1+2.5\phi_f}\exp(B\phi_f) \tag{19}$$

where ϕ_f is the volume fraction of filler and σ_{yc} and σ_{ym} denote the tensile yield stresses of the composite and matrix,

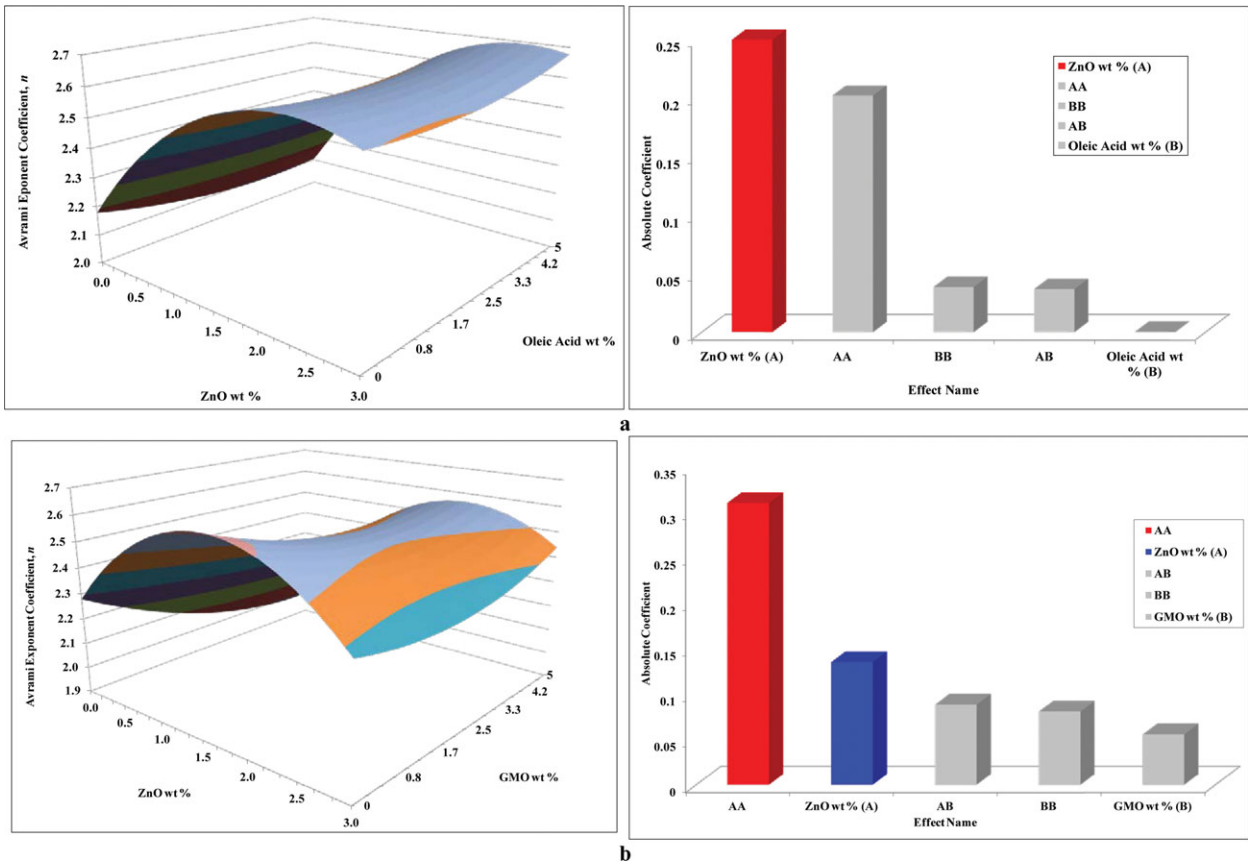

Figure 10. Graphical representation of the regression analysis of n of the composite films depending on the additive concentration: (a) ZnO–oleic acid and (b) ZnO–GMO. [Color figure can be viewed in the online issue, which is available at wileyonlinelibrary.com.]

Table IX. Mechanical Properties and Polymer–Inorganic Additive *B* Values Calculated from the Pukanszky Model of the PCL Films

Sample	Tensile strength (MPa)	Elongation at break (%)	Young's modulus (MPa)	*B*
Neat PCL	9.75	592.69	128.00	
PCL-O1	8.55	559.08	95.10	−7.34
PCL-O3	13.05	703.23	117.80	4.87
PCL-O5	9.40	699.20	108.50	0.95
PCL-G1	17.81	730.91	125.00	16.21
PCL-G3	11.87	668.21	138.00	3.05
PCL-G5	14.28	705.94	109.90	2.40
PCL-Z0.1	8.67	93.41	89.20	-468.86
PCL-Z0.1-O1	8.52	66.96	100.10	4.60
PCL-Z0.1-O3	8.38	90.18	95.00	0.96
PCL-Z0.1-O5	7.45	130.13	79.20	-1.86
PCL-Z0.1-G1	18.46	785.50	115.00	10.60
PCL-Z0.1-G3	15.05	678.66	85.60	0.39
PCL-Z0.1-G5	11.68	334.40	116.60	2.69
PCL-Z1	8.13	83.57	122.20	7.70
PCL-Z1-O1	9.71	205.24	107.10	−2.03
PCL-Z1-O3	12.94	372.37	106.90	1.57
PCL-Z1-O5	10.01	328.99	104.30	−1.36
PCL-Z1-G1	13.63	462.34	140.60	3.81
PCL-Z1-G3	11.29	243.59	99.00	3.68
PCL-Z1-G5	10.23	258.83	94.00	1.16
PCL-Z3	9.83	188.05	105.30	−3.18
PCL-Z3-O1	8.19	159.19	85.40	−0.82
PCL-Z3-O3	9.76	71.56	92.10	0.50
PCL-Z3-O5	10.16	204.71	101.20	2.48
PCL-Z3-G1	10.15	188.91	105.10	3.17
PCL-Z3-G3	9.31	253.34	91.10	−2.48
PCL-Z3-G5	7.63	105.97	77.50	−2.20

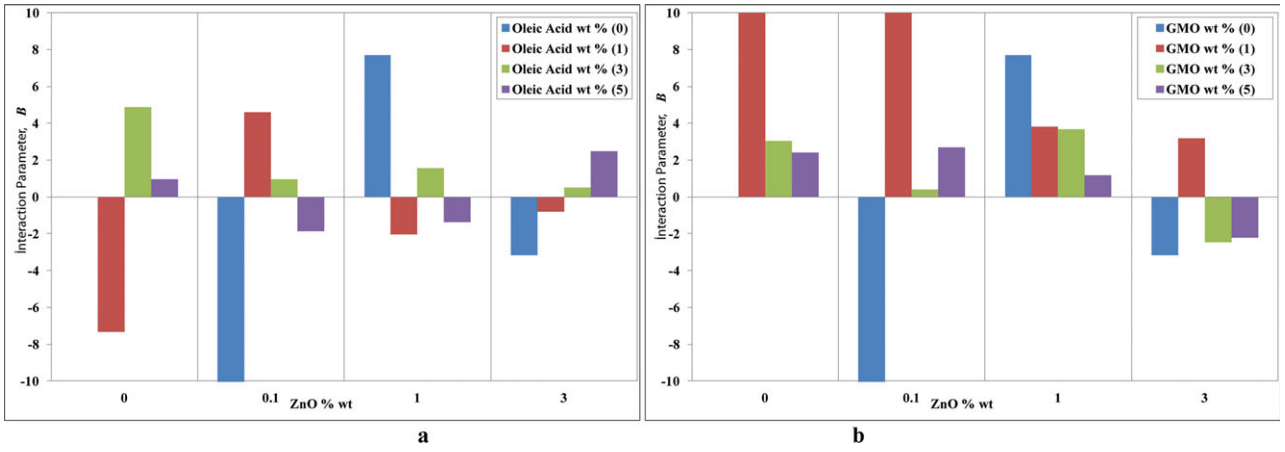

Figure 11. Effect of the organic additive on the polymer–filler interaction according to the interaction parameter: (a) ZnO–oleic acid and (b) ZnO–GMO. [Color figure can be viewed in the online issue, which is available at wileyonlinelibrary.com.]

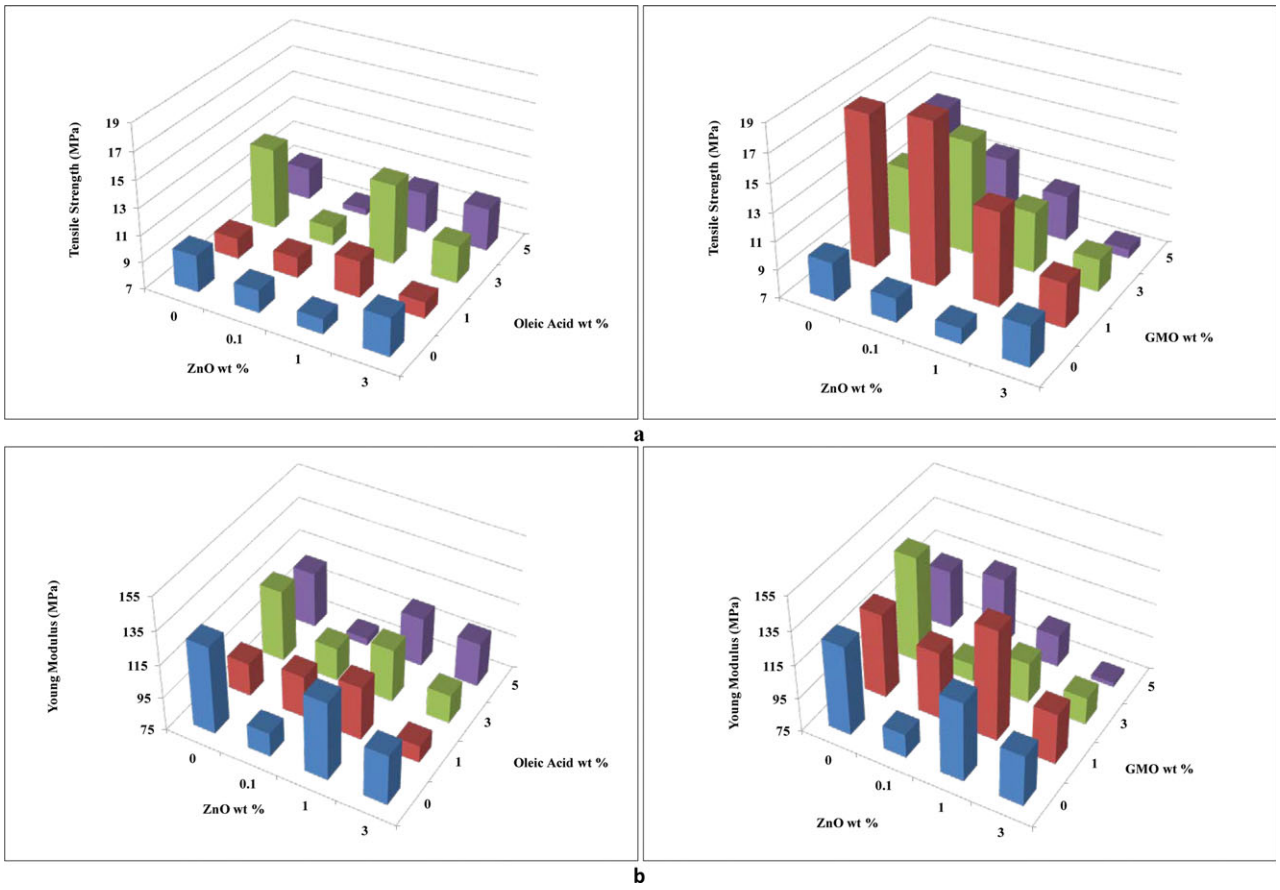

Figure 12. Effect of the additives on the mechanical properties of the PCL composite films: (a) tensile strength and (b) Young's modulus. [Color figure can be viewed in the online issue, which is available at wileyonlinelibrary.com.]

respectively. The first term in eq. (19) is related to the decrease in the effective load-bearing cross section, and the second one is concerned with the interfacial interaction between the filler and the matrix. The interfacial interaction depends on the area of the interphase and the strength of the interaction, as shown in eq. (20):

$$B = (1 + A_f \rho_f t)\ln(\sigma_{yi}/\sigma_{ym}) \tag{20}$$

where t, σ_{yi}, A_f, and ρ_f are the thickness of the interface, the strength of the interaction, the specific surface area, and the density of the filler, respectively.

The Young's modulus, tensile strength, percentage elongation at break, and B [calculated from eq. (20)] of the PCL composite films are given in Table VIII. Parameter B in the model characterizes the interaction between PCL and ZnO, and the higher B values indicate better interaction. Negative B values can be an indication of a nonhomogeneous distribution of additives in the composites and result from weak adhesion at the interface of the polymer and additive. For the PCL–ZnO composite film without the organic additive, the value of B had the highest negative value (−468.86); this reflected the worst dispersion, as shown in Table IX. This value was left out in Figure 11 for the benefit of the scale observation. As shown in Figure 11, with the absence of oleic acid or GMO, the ZnO particles were not dispersed homogeneously in the PCL matrix.

The measured tensile strength changed between 7.45 and 18.46 MPa. The addition of ZnO decreased the tensile strength. According to Figure 12(a), the tensile strength values show a decreasing trend; this behavior was due to the interactions between the ZnO particles as more agglomerates were formed. The addition of organic additives improved the dispersion. The percentage elongation at break of the PCL composite film with 0.1 wt % ZnO and 1 wt % GMO was observed as the highest value. The values of Young's modulus changed between 77.50 and 140.60 MPa. The values of Young's modulus of the PCL composite films with different additives changed in the range of 20–2920 MPa.[7,32,48–50] The values of Young's modulus of the composite films were consistent with values from the literature. Inorganic additives increased Young's modulus of the PCL composite films. Similarly, ZnO also increased Young's modulus of the composite films. The increase in Young's modulus of the ZnO-filled composites indicated an increase in the rigidity of PCL related to the restriction of the mobility of the PCL matrix due to the presence of the fillers. The obtained composite films were strong and had a high percentage of elongation as a new material.

CONCLUSIONS

The effects of ZnO, oleic acid, and GMO on the crystallization and mechanical behavior of PCL were studied by DSC, X-ray diffraction, and tensile tests. The isothermal DSC results were analyzed by the Avrami model. The Avrami model indicated that the crystallization was controlled by nucleation, and the crystals had a spherical structure. The nucleation type changed between thermal and athermal nucleation processes and was followed by three-dimensional crystal growth. X-ray diffraction also showed that when the additives were used alone, both the crystal thickness and degree of crystallinity decreased at low concentrations and increased at high concentrations of ZnO. The DSC and XRD results revealed that ZnO acted as nucleating agent, and oleic acid and GMO acted as plasticizers and crystallization modifiers. The mechanical tests revealed that the composite films were ductile and quite strong. *B* indicated that the organic additives provided a good dispersion of ZnO. The determination of the relation between the crystallinity and product properties, such as the structural and mechanical properties, and the isothermal crystallization kinetics was the aim of this study. The properties of these new composite materials can be tailored as required for tissue engineering, bone implants, root canal fillings in dental applications, controlled drug delivery, and food packaging applications.

ACKNOWLEDGMENTS

This work was supported by the Scientific and Technological Research Council of Turkey (contract grant number TUBİTAK-110M157) and Ege University Scientific Research Project Fund (project BAP 09/MÜH/093).

REFERENCES

1. Woodruff, M. A.; Hutmacher, D. W. *Prog. Polym. Sci.* **2010**, *35*, 1217.
2. Chung, T. C.; Rhubright, D. *Macromolecules* **1994**, *27*, 1313.
3. Seretoudi, G.; Bikiaris, D.; Panayiotou, C. *Polymer* **2002**, *43* 5405.
4. Tjong, S. C.; Xu, Y.; Meng, Y. Z. *Polymer* **1999**, *40*, 3703.
5. Diba, M.; Fathi, M. H.; Kharaziha, M. *J Mater. Lett.* **2011**, *65*, 1931.
6. Bugatti, V.; Costantino, U.; Gorrasi, G.; Nocchetti, M.; Tammaro, L.; Vittoria, V. *J. Eur. Polym. J.* **2010**, *46*, 418.
7. Furman, B. R.; Wellinghoff, S. T.; Laine, R. M.; Chan, K. S.; Nicolella, D. P.; Rawls, H. R. *J. Appl. Polym. Sci.* **2009**, *114*, 993.
8. Alani, A.; Knowles, J. C.; Chrzanowski, W.; Ng, Y.-L.; Gulabivala, K. *Dent. Mater.* **2009**, *25*, 400.
9. Wu, C. S. *J. Appl. Polym. Sci.* **2004**, *92*, 1749.
10. Oliveira, A. L.; Costa, S. A.; Sousa, R. A.; Reis, R. L. *Acta Biomater.* **2009**, *5*, 1626.
11. Homminga, D.; Goderis, B.; Dolbnya, I.; Groeninckx, G. *Polymer* **2006**, *47*, 1620.
12. Fukushima, K.; Abbate, C.; Tabuani, D.; Gennari, M.; Rizzarelli, P.; Camino, G. *J. Mater. Sci. Eng. C* **2010**, *30*, 566.
13. Ludueña, L. N.; Vazquez, A.; Alvarez, V. A. *J. Appl. Polym. Sci.* **2008**, *109*, 3148.
14. Liu, H.; Huang, Y.; Yuan, L.; He, P.; Cai, Z.; Shen, Y.; Xu, Y.; Yu, Y.; Xiong, H. *Carbohydr. Polym.* **2010**, *79*, 513.
15. César, M. E. F.; Mariani, P. D. S. C.; Innocentini-Mei, L. H.; Cardoso, E. J. B. N. *Polym. Test.* **2009**, *28*, 680.
16. Rosa, D. S.; Guedes, C. G. F.; Casarin, F. *Polym. Bull.* **2005**, *54*, 321.
17. Mitchell, C. A.; Krishnamoorti, R. *Polymer* **2005**, *46*, 8796.
18. Dem'yanets, L. N.; Li, L. E.; Uvarova, T. G.; Mininzon, Y. M. *Inorg. Mater.* **2011**, *44*, 40.
19. Lepot, N.; Van Bael, M. K.; Van den Rul, H.; D'Haen, J.; Peeters, R.; Franco, D.; Mullens, J. *J. Appl. Polym. Sci.* **2011**, *120*, 1616.
20. Li, Y.; Wu, K.; Zhitomirsky, I. *Colloids Surf. A* **2010**, *356*, 63.
21. Ma, X.; Chang, P. R.; Yang, J.; Yu, J. *Carbohydr. Polym.* **2009**, *75*, 472.
22. Sui, X.; Shao, C.; Liu, Y. *Polymer* **2007**, *48*, 1459.
23. Kim, H.-W. *J. Biomed. Mater. Res. A* **2007**, *83*, 169.
24. Olson, J. R. U.S. Pat. 5,610,214 (**1997**).
25. Montgomery, D. C. Design and Analysis of Experiments, 5th ed.; Wiley: New York, **2001**; p 697.
26. Hansen, C. M. Hansen Solubility Parameters: A User's Handbook; CRC: Boca Raton, FL, **2007**.
27. Stefanis, E.; Panayiotou, C. *Int. J. Thermophys.* **2008**, *29*, 568.
28. Patterson, A. L. *Phys. Rev.* **1939**, 56.
29. Bittiger, H.; Marchessault, R. H. *Acta Cryst. Sect. B* **1923**, 26.
30. Hammond, C. The Basics of Crystallography and Diffraction; Oxford University Press: New York, **2009**.
31. Lepoittevin, B.; Devalckenaere, M.; Pantoustier, N.; Alexandre, M.; Kubies, D.; Calberg, C.; Jerome, R.; Dubois, P. *Polymer* **2002**, *43*, 4017.
32. Shieh, Y. T.; Lai, J. G.; Tang, W. L.; Yang, C. H.; Wang, T. L. *J. Supercrit. Fluids* **2009**, *49*, 385.
33. Joseph, S. C.; Prashanth, H. K. V.; Rastogi, N. K.; Indiramma, A. R.; Reddy, Y. S.; Raghavarao, K. S. M. S. *Food Bioprocess. Technol.* **2009**, *4*, 1179.
34. Gedde, U. W. Polymer Physics; Chapman & Hall: London, **1995**.
35. Zhu, G.; Xu, Q.; Qin, R.; Yan, H.; Liang, G. *Radiat. Phys. Chem.* **2005**, *74*, 42.
36. Sasaki, T. J. *Therm. Anal. Calorim.* **2012**.
37. Barman, S.; Vasudevan, S. *J. Phys. Chem. B* **2006**, *110*, 651.
38. Deshmukh, G. S.; Pathak, S. U.; Peshwe, D. R.; Ekhe, J. D. *Bull. Mater. Sci.* **2010**, *33*, 277.
39. Rodriguez, F. Principles of Polymer Systems; McGraw-Hill: Singapore, **1987**.
40. Janeschitz, K. H. Crystallization Modalities in Polymer Melt Processing: Fundamental Aspects of Structure Formation; Springer: Germany, **2009**.

41. Di Maio, E.; Iannace, S.; Sorrentino, L.; Nicolais, L. *Polymer* **2004**, *45*, 8893.
42. Dhanvijay, P. U.; Shertukde, V. V. *Polym.-Plast. Technol. Eng.* **2011**, *50*, 1289.
43. Ratta, V. Ph.D Thesis, Virginia Polytechnic Institute, **1999**.
44. Run, M.; Wang, Y.; Yao, C.; Gao, J. *Thermochim. Acta* **2006**, *447*, 13.
45. Guo, Q.; Groeninckx, G. *Polymer* **2001**, *42*, 8647.
46. Skoglund, P.; Fransson, A. *J. Appl. Polym. Sci.* **1996**, *61*, 2455.
47. Metin, D.; Tihminlioğlu, F.; Balköse, D.; Ülkü, S. *Compos. A* **2004**, *35*, 23.
48. Yu, H.; Matthew, H. W.; Wooley, P. H.; Yang, S. Y. *J. Biomed. Mater. Res. Part B* **2008**, *86*, 541.
49. Yu, Z.; Yin, J.; Yan, S.; Xie, Y.; Ma, J.; Chen, X. *Polymer* **2007**, *48*, 6439.
50. Wu, K. J.; Wu, C. S.; Chang, J. S. *Process. Biochem.* **2007**, *42*, 669.